

Monte Carlo study of multicomponent monolayer adsorption on square lattices

G. D. García ^{a,b}, F. O. Sánchez-Varretti ^{a,b}, F. Bulnes ^a,
A. J. Ramirez-Pastor ^{a,1}

^a*Dpto. de Física, Instituto de Física Aplicada, Universidad Nacional de San Luis - CONICET, Chacabuco 917, 5700 San Luis, Argentina.*

^b*Universidad Tecnológica Nacional, Regional San Rafael, Gral. Urquiza 314, 5600, San Rafael, Mendoza, Argentina.*

Abstract

The monolayer adsorption process of interacting binary mixtures of species A and B on square lattices is studied through grand canonical Monte Carlo simulation in the framework of the lattice-gas model. Four different energies have been considered in the adsorption process: 1) ϵ_0 , interaction energy between a particle (type A or B) and a lattice site; 2) w_{AA} , interaction energy between two nearest-neighbor A particles; 3) w_{BB} , interaction energy between two nearest-neighbor B particles; 4) $w_{AB} = w_{BA}$, interaction energy between two nearest-neighbors being one of type A and the other of type B . The adsorption process has been monitored through total and partial isotherms and differential heats of adsorption corresponding to both species of the mixture. Our main interest is in the repulsive lateral interactions, where a variety of structural orderings arise in the adlayer, depending on the interaction parameters (w_{AA} , w_{BB} and w_{AB}). At the end of this work, we determine the phase diagram characterizing the phase transitions occurring in the system. A nontrivial interdependence between the partial surface coverage of both species is observed.

Key words: Equilibrium thermodynamics and statistical mechanics, Surface thermodynamics, Adsorption isotherms, Monte Carlo simulations

¹ Corresponding author. Fax +54-2652-430224, E-mail: antorami@unsl.edu.ar

1 Introduction

The adsorption process of mixture gases on solid surfaces is a topic of great interest not only from an intrinsic but also from a technological point of view, due to its importance for new developments in fields like gas separation and purification [1,2,3,4]. Although this problem has been theoretically [5,6,7,8,9,10,11,12] and experimentally [11,12,13,14,15] studied for many years, some aspects are still unclear being necessary to reach a better understanding about the behavior of the adsorbate during the adsorption process of the mixture.

As in any adsorption process, a complete analysis of the behavior of gas molecules under the influence of an adsorbent requires the knowledge of the forces of molecular interactions [1,16,17,18]. In other words, the description of real multicomponent adsorption requires to take into account the effect of the lateral interactions between each species of the mixture. An exact treatment of this problem, including ad-ad interactions, is unfortunately not yet available and, therefore, the theoretical description of adsorption relies on simplified models [4]. One way of overcoming this complication is to use Monte Carlo (MC) simulation method [19,20,21,22,23]. MC technique is a valuable tool for studying surface molecular processes, which has been extensively used to simulate many surface phenomena including adsorption [24], diffusion [25], reactions, phase transitions [26], etc.

In this line of work, a previous article was devoted to the study of the adsorption of interacting binary mixtures on triangular lattices [27]. In Ref. [[27]], Rinaldi et al. obtained adsorption isotherms and differential heats of adsorption corresponding to both species of the mixture, for different values of the lateral interactions between the adsorbed species. An unusual feature was observed when (*i*) the lateral interaction between A and B particles was different from zero, and (*ii*) the initial concentration of B particles was in the range [0.3, 0.5]. In these conditions, the A particles adsorbing on the lattice expel the B adsorbed particles; then, the partial A [B] coverage increases [decreases]. During this regime the number of desorbed particles is greater than the number of adsorbed particles which results in a decreasing of the total coverage that occurs for a wide range in values of chemical potential where the slope of the adsorption isotherm is negative. The behavior of the system was fully explained through the analysis of the phase diagrams for order-disorder transitions occurring in the adsorbed layer.

Because the structure of lattice space plays a fundamental role in determining the statistics of mixtures, it is of interest and of value to inquire how a specific lattice structure influences the main thermodynamic properties of adsorbed mixtures. In this context, the objectives of the present paper are (1) to extend

the previous work to square lattices using the same techniques developed in Ref. [[27]] and (2) to study the effect of the lattice structure on the adsorption of interacting binary mixtures. For this purpose, multicomponent gases adsorbed on square lattices are studied by using grand canonical ensemble MC simulation. The process was analyzed by following total and partial adsorption isotherms as well as differential heats of adsorption corresponding to both species of the mixture. The detailed behavior of these quantities will be shown to be directly related to the phase diagrams of the system.

The outline of the paper is as follows. In Sec. II we describe the lattice-gas model and the simulation scheme. In Sec. III we present the MC results. Finally, the general conclusions are given in Sec. VI.

2 Lattice-Gas Model and Monte Carlo Simulations

The adsorptive surface is represented by a two-dimensional square lattice of $M = L \times L$ adsorption sites, with periodic boundary conditions. The substrate is exposed at a temperature T to an ideal gas phase consisting of a binary mixture of particles A and B with chemical potentials μ_A and μ_B , respectively. Particles can be adsorbed on the lattice with the restriction of at most one adsorbed particle per site and we consider a nearest-neighbor (NN) interaction energy w_{XY} ($X, Y = A, B$) among them. The adsorbed phase is then characterized by the Hamiltonian:

$$H = \frac{1}{2} \sum_i^M \sum_{l \in \{NN, i\}} [w_{AA} \delta_{c_i, c_l, 1} + w_{BB} \delta_{c_i, c_l, -1} + w_{AB} (\delta_{c_i, 1} \delta_{c_l, -1} + \delta_{c_i, -1} \delta_{c_l, 1})] + \epsilon_0 \sum_i^M (\delta_{c_i, 1} + \delta_{c_i, -1}) - \sum_i^M (\mu_A \delta_{c_i, 1} + \mu_B \delta_{c_i, -1}) \quad (1)$$

where c_i is the occupation number of site i ($c_i = 0$ if empty; $c_i = 1$ if occupied by A and $c_i = -1$ if occupied by B); $l \in \{NN, j\}$ runs on the four NN sites of site i ; the δ 's are Kronecker delta functions and ϵ_0 is the interaction energy between a monomer (type A or B) and a lattice site. In this contribution, the chemical potential of one of the components is fixed throughout the process ($\mu_B = 0$), while the other one (μ_A) is variable, as it is usually assumed in studies of adsorption of gas mixtures [28]. In the actual implementation of the model ϵ_0 was set equal to zero, without loss of any generality.

With respect to the computational simulations, the Monte Carlo procedure used has been discussed in detail in Ref. [[27]] and need not be repeated here. In this case, the first 10^6 Monte Carlo steps (MCS) were discarded to allow equilibrium, while the next 10^6 MCS were used to compute averages.

3 Results and discussion

The computational simulations have been developed for square $L \times L$ lattices, with $L = 96$, and periodic boundary conditions. With this lattice size we verified that finite-size effects are negligible. Note, however, that the linear dimension L has to be properly chosen such that the adlayer structure is not perturbed.

In order to understand the basic phenomenology, we consider in the first place the case of single-gas adsorption. This was achieved by making $\mu_B \rightarrow -\infty$. Fig. 1 shows the behavior of the adsorption isotherms and the differential heats of adsorption for different strengths of repulsive interparticle interactions. As expected, we obtain the well-known Langmuir isotherm passing through the point $(\mu_A/k_B T = 0, \theta_A = 1/2)$ when $w_{AA}/k_B T = 0$ (being k_B the Boltzmann constant). Two features, which are useful for the analysis of mixed-gas adsorption, are worthy of comment: (a) as the NN repulsive interaction is increased, the coverage at zero chemical potential decreases and asymptotically approaches $\theta_A = 0.226$; (b) as the repulsive NN interaction passes a critical value $w_c/k_B T \approx 1.763$ [29,30], a plateau develops in the isotherm at $\theta_A = 1/2$ indicating the appearance of $c(2 \times 2)$ ordered phase on the surface. In what follows, we consider mixed-gas adsorption but keeping species B at a fixed value of the chemical potential $\mu_B/k_B T = 0$. In addition, we have considered $k_B T = 1$ for simplicity, without any loss of generality.

We start with the case of a binary mixture in the presence of repulsive lateral interactions between the particles. The effect of AA interactions is depicted in Fig. 2, where $w_{AA}/k_B T \neq 0$, $w_{AB}/k_B T = 0$ and $w_{BB}/k_B T = 0$. We have plotted the partial (a) and total (b) adsorption isotherms, and the differential heats of adsorption corresponding to the species A (c) and B (d). It can be observed in Fig. 2 (a) and (b), that the initial coverage takes the same value $\theta = 0.5$ for all isotherms; this behavior can be explained as follows: for $\mu_A/k_B T \rightarrow -\infty$ the A particle coverage is zero while the B particles are randomly distributed on the lattice with θ_B given by the Langmuir isotherm $\theta_B = \exp(\mu_B/k_B T)/[1 + \exp(\mu_A/k_B T) + \exp(\mu_B/k_B T)]$, which for $\mu_B/k_B T = 0$ is $\theta = \theta_B = 1/2$.

As discussed above, for a lattice gas of interacting monomers adsorbed on a square surface, there exists a critical interaction ($w_c/k_B T \approx 1.763$) corresponding to a phase transition in the adsorbate. The nearest-neighbor coupling, w , determines the character of the phase transition: (i) if $w < 0$ (attractive case) the system exhibits a first-order phase transition, and (ii) for $w > 0$ (repulsive case) a continuous order-disorder phase transition occurs in the adsorbate, which is observed as a clear plateau in the adsorption isotherms. Following this behavior, a well-defined and pronounced step appears in the partial isotherms

as the interaction $w_{AA}/k_B T$ is increased. Thus, the interaction between A molecules determines a $c(2 \times 2)$ ordered phase for such particles. Therefore, the A isotherm presents a plateau at half coverage [see Fig. 2(a)]. At equilibrium, the B particles occupy half of the empty sites, and the corresponding B isotherm presents a plateau at $\theta_B = 0.25$; this behavior is a consequence of the excluded volume but is not due to the interactions. The total isotherm [Fig. 2(b)] is the sum of the partial isotherms, then the plateau appears at $\theta = 0.75$.

In Fig. 2(c), the differential heat of adsorption q_A corresponding to the A species is plotted versus θ_A . The behavior of the curves can be explained by analyzing two different adsorption regimes: (i) for $0.5 < \theta < 0.75$ ($0 < \theta_A < 0.5$), the ad-molecules avoid NN occupancy which produces $q_A \approx 0$ (as for $w_{AA}/k_B T = 0$), and (ii) for $0.75 < \theta < 1$ ($0.5 < \theta_A < 1$), the adsorption of one more molecule involves an increment cw_{AA} in the energy of the system, where c is the lattice connectivity (in this case, $c = 4$). The maximum in q_A for $\theta \rightarrow 0.75^-$ corresponds to the critical coverage at which a dramatic change of order takes place in the system (the system passes from the disordered to the ordered phase [31]). A similar situation occurs for the minimum in q_A at $\theta \rightarrow 0.75^+$.

The adsorption of the A species induces an interesting behavior in the B isotherm, which also exhibits well-defined steps although the B particles do not interact neither with B particles nor with A particles ($w_{AB}/k_B T = 0$ and $w_{BB}/k_B T = 0$). This behavior is a consequence of the excluded volume but is not due to the interactions. Then, as it is expected, q_B is strictly zero over all the coverage range [see Fig. 2 d)].

We now continue the study of the effect of AA interactions with $w_{AB}/k_B T = 0$ and $w_{BB}/k_B T = 2$ (Fig. 3), therefore introducing BB interactions; $w_{AB}/k_B T = 2$ and $w_{BB}/k_B T = 0$ (Fig. 4) introducing interspecies interactions (and removing BB interactions) and, finally, we analyze $w_{AB}/k_B T = 2$ and $w_{BB}/k_B T = 2$ (Fig. 5) where all interactions are present.

In the case of Fig. 3, the behavior of the partial [Fig. 3 a)] and total [Fig. 3 b)] isotherms and the differential heat of adsorption q_A [Fig. 3 c)] is similar to those in Fig. 2. The main difference is associated to the value of θ_B at low pressures (which is lower than 0.5), and to the behavior of q_B that is not zero any more.

Clearly, for $w_{AA}/k_B T = 0$, A particles are distributed at random and B particles start from a low coverage (close to 0.226, as explained in Fig. 1) which rapidly decreases as more A particles are adsorbed. Therefore as the total coverage increases, B particles interact with each other less frequently and q_B increases steadily. However, as $w_{AA}/k_B T$ becomes sufficiently high so that an

ordered phase is formed, a sudden increase in q_B is produced due to a sudden increase in the screening effect between B particles produced by A particles.

An unusual feature is observed in the case of Fig. 4: as $\mu_A/k_B T$ increases and A particles start to adsorb, B particles are displaced from the surface so that the total A + B coverage decreases and shows a local minimum [Fig. 4 b)]. This effect, which has been previously called *mixture effect* [27], can be explained as follows: as the coverage of A particles is sufficiently high so that AB interactions occur, the repulsive character of w_{AB} leads to more B particles being displaced from the surface than A particles being adsorbed on the surface.

The mixture effect is clearly reflected in the behavior of q_A [Fig. 4 c)] and q_B [Fig. 4 d)]. In fact, for $0 < \theta_A < 1/2$, A particles do not interact with other A or B molecules and, consequently, $q_A = q_B = 0$ (see insets). The $c(2 \times 2)$ phase of A particles starts to develop and is completed at $\theta_A = 1/2$. For $1/2 < \theta_A$, A particles fill the vacancies. In this regime, the coverage of B particles tends to zero and does not perturb significantly the adsorption of the A species. The important fluctuations in q_B are clear signals that the number of B particles is practically zero.

Our simulations show how the competition between two species in presence of repulsive mutual interactions reinforces the displacement of one species by the other and leads to the presence of the mixture effect. To complete this analysis, it is interesting to note that the mixture effect [also called adsorption preference reversal (APR) phenomenon] has also been observed for methane-ethane mixtures [7,8,9,10]. The rigorous results presented in Ref. [[10]] showed that, in the case of methane-ethane mixtures, the APR is not a consequence of the existence of repulsive interactions between the ad-species, but it is the result of the difference of size (or number of occupied sites) between methane and ethane. A similar scenario has been observed for different mixtures of linear hydrocarbons in silicalite [12], carbon nanotube bundles [33] and metal-organic frameworks [34].

In the case of Fig. 5, the presence of repulsive BB interactions results in a initial coverage of B particles close to 0.226. This small fraction of B molecules does not perturb significantly the adsorption of the A species and the mixture effect disappears. This finding indicates that, in addition to the requirements of repulsive lateral interactions between the two species, the amount of particles on the surface is essential for the existence of the mixture effect. The rest of the figure can be understood following the arguments given above.

In the following we study the effects of variable AB interactions as shown in Figs. 6 to 9. We start with the case where $w_{AA}/k_B T = w_{BB}/k_B T = 0$ (Fig. 6). Here no ordered phases are formed and for sufficiently high $w_{AB}/k_B T$ an

important mixture effect appears. Let us choose for our analysis the curves corresponding to $w_{AB}/k_B T = 1$. B coverage is initially 0.5. As A molecules are adsorbed B molecules are eliminated from the surface in such a way that θ decreases. At the same time q_A starts at a low value and increases rapidly (with a bivaluated behavior) tending to 0 as $\theta \rightarrow 1$, while q_B starts near 0 and tends to $4w_{AB}$ as $\theta \rightarrow 1$. As soon as BB interactions are added, the starting B coverage is ~ 0.226 and the mixture effect disappears (Fig. 7). In the presence of AA and AB interactions (Fig. 8), $w_{AB}/k_B T = 0.5$ is sufficiently high for the appearance of ordered phases for A molecules, so that the resulting behavior is similar to that of Fig. 4. The inclusion of the three interactions (Fig. 9), only produces the elimination of the mixture effect, compared to Fig. 8, due to the low initial B coverage.

The effect of variable BB interactions is discussed in Figs. 10 to 13. Different cases were considered: $w_{AA}/k_B T = w_{AB}/k_B T = 0$ (Fig. 10); $w_{AA}/k_B T = 0$ and $w_{AB}/k_B T = 2$ (Fig. 11); $w_{AA}/k_B T = 5$ and $w_{AB}/k_B T = 0$ (Fig. 12) and $w_{AA}/k_B T = 5$ and $w_{AB}/k_B T = 2$ (Fig. 13). Given the value of the parameters in Fig. 10, neither the coverage of A [Fig. 10 a)] nor the differential heat of adsorption [Fig. 10 c)] are affected by BB interactions. As discussed in Fig. 1, the coverage of B at low pressure starts at 0.5 and decreases as $w_{BB}/k_B T$ increases towards the limiting value of 0.226 [see Fig. 10 a)]. However, the coverage of B does not present any special features. Such a special feature does indeed appear in the behavior of q_B [Fig. 10 d)], which decreases steadily as $w_{BB}/k_B T$ increases below a certain critical value, $w_{BB}^c/k_B T$ (being $w_{BB}^c/k_B T \approx 2$), and increases above it. The explanation for this behavior is that B particles adsorb more or less at random below $w_{BB}^c/k_B T$, thereby allowing some BB interactions which contribute to the decrease in the differential heat of adsorption. Above $w_{BB}^c/k_B T$, B particles adsorb forming an ordered structure so that BB interactions stop contributing and q_B increases. The condition $w_{AB}/k_B T = 0$ restricts the possibility of mixture effect.

In Fig. 11, the presence of AB interactions favors the displacement of B particles and, consequently, the slopes of the B partial isotherms are increased. On the other hand, as the initial fraction of B particles is high ($0.3 \leq \theta_B^i \leq 0.5$), which occurs for small values of $w_{BB}/k_B T$ ($0 \leq w_{BB}/k_B T \leq 0.5$), AB interactions lead to mixture effect. In a wide range of coverage, $0.4 \leq \theta \leq 1$, the curves in Fig. 11 are very similar between them (this is clearly visualized in the case q_A and q_B), which is indicative of the rapid decreasing of the number of B particles on the surface.

In Fig. 12, the adsorption of A particles [Fig. 12 a)] follows a unique isotherm and is independent of the strength of BB interactions. Adsorption of B particles decreases at low A coverage with increasing values of $w_{BB}/k_B T$ and tends to the limiting value $\theta_B = 0.226$. However, at high A coverage all isotherms tend to that corresponding to $w_{BB}/k_B T = 0$ because there are no NN vacant

sites in that range available for the adsorption of B particles. This determines the total coverage behavior shown in Fig. 12 b). The curves of q_A , shown in Fig. 12 c), present a very similar behavior between them. This is, one marked jump appears, corresponding to the plateau in A isotherms. In contrast, q_B presents two types of behaviors [Fig. 12 d)]. Thus, at very low $w_{BB}/k_B T$ values (negligible interactions) and very high $w_{BB}/k_B T$ values (above the critical value for the formation of the ordered phase), it remains practically constant, while at intermediate values it increases in line with the total coverage. In the last case (Fig. 13), the adsorption process can be easily understood: the B particles disappear for low values of $\mu_A/k_B T$. Then, for higher $\mu_A/k_B T$'s, all curves collapse on a unique curve.

3.1 Phase diagrams

In order to rationalize the results presented in previous section, we will determine the temperature-coverage phase diagram characterizing our system in the range of the parameters studied. The curves will be obtained as a generalization of the well-known phase diagram for a lattice-gas of repulsive monomers adsorbed on a homogeneous square lattice, which is shown in Fig. 14.

Some of the exact properties of this system have been found, especially by Onsager [35]. These are confined mostly to the special condition $\theta = 1/2$, but by symmetry, it can be deduced that $\theta_c = 1/2$, if a critical point exists, so this is the most interesting value of θ . Thus, the maximum of the coexistence curve (occurring to $\theta = 1/2$) corresponds to a critical value $k_B T_c/w_{AA} = [2 \ln(\sqrt{2} - 1)]^{-1} \approx 0.567$ [29,30]. On the other hand, zones I, II and III correspond to a disordered lattice-gas state, a ordered state [$c(2 \times 2)$ phase], and a disordered lattice-liquid state, respectively.

We start with the analysis of Fig. 13, where our model is almost identical to a lattice-gas of one species. As indicated in Fig. 13, the existence of repulsive AB interactions favors the displacement of B particles. Once $\theta_B \approx 0$, which occurs at $\mu_A/k_B T \approx 5$, the binary mixture is equivalent to the square lattice-gas of one species. To corroborate this affirmation, Fig. 15 shows the total isotherms of Fig. 13 b) (symbols), in comparison with the adsorption isotherm corresponding to a square lattice-gas of one species and $w_{AA}/k_B T = 5$ (solid line). The analysis can be separated in two parts: for $\theta < 1/2$, there exist B particles on the lattice and, consequently, the curves of the mixture deviate from that corresponding to one species. For $\theta > 1/2$, the coverage of B particles is negligible and all curves collapse on a unique curve. Then, the phase diagram characterizing a binary mixture with the set of parameters of Fig. 13 is identical to that shown in Fig. 14. The unique difference with the one-species phase diagram is that the zone I now corresponds to an A-B mixture with different

proportions according to the value of $w_{BB}/k_B T$.

As a basis for the analysis of the behavior of the system for variable $w_{AB}/k_B T$, we begin by considering one of the cases of Fig. 13 (that corresponding to $w_{BB}/k_B T = 0$), which is characterized by a phase diagram as shown in Fig. 14. This behavior is representative of systems with high values of $w_{AB}/k_B T$ (in the range $w_{AB}/k_B T \geq 2.0$), as is indicated in Fig. 16 (see the plane corresponding to $w_{AB}/k_B T = 2.0$). As $w_{AB}/k_B T$ is decreased, the maxima of the coexistence curves in zone II shift to higher values of coverage². This can be better visualized in Fig. 17 (solid circles, bottom axis), where we plot the densities corresponding to the maxima of the coexistence curves in zone II, θ_c 's, as a function of $w_{AB}/k_B T$. The figure allows to analyze the behavior of a binary mixture with $w_{BB}/k_B T = 0$, variable $w_{AB}/k_B T$ and $w_{AA}/k_B T$ in the critical regime. The curves can be understood according to the following reasoning. As it was explained for high values of the AB lateral interaction, the zone II corresponds to a phase of A particles. As $w_{AB}/k_B T$ decreases, the phase is complemented with B particles, which are randomly distributed in the empty sites of the structure. As a typical example, we will analyze the case of $w_{BB}/k_B T = w_{AB}/k_B T = 0$. In this case, the B particles, which are at chemical potential $\mu_B/k_B T = 0$, occupy at random 1/2 of the empty sites of the phase³. Then, the phase corresponding to zone II is formed by a structure of A particles (which occupy 1/2 of the total sites) complemented with B particles (which occupy at random 1/4 of the total sites). The resulting value of θ_c is 3/4. The rest of the points in Fig. 17 can be explained by similar arguments.

We now turn to the effect of BB interactions (see Fig. 17, open circles, upper axis). For this purpose, we set $w_{AB}/k_B T = 0$ and $w_{AA}/k_B T$ in the critical regime. The adsorption properties corresponding to this case were discussed in Fig. 12. We start the analysis with the case $w_{BB}/k_B T = w_{AB}/k_B T = 0$, where $\theta_C = 3/4$. As $w_{BB}/k_B T$ is increased, θ_C remains constant. In this case, the phase corresponds to a $c(2 \times 2)$ phase of A particles complemented with a partial coverage of B particles equal to 1/4.

Figs. 14-17 allow to characterize the critical behavior of a binary mixture adsorbed in a square lattice in the region of the parameters studied in the present contribution. Namely:

- In Fig. 2, the total isotherms have a pronounced plateau at $\theta = 3/4$ for strongly repulsive AA interactions, which smoothes out already for $w_{AA}/k_B T <$

² The figure shows the upper part of each coexistence curve. A complete analysis of the curve should require a more complex study (percolation of phase, zero-temperature calculations, etc.), which are out of the scope of the present paper.

³ Note that 1/2 of the empty sites of the phase $c(2 \times 2)$ represents 1/4 of the total sites.

1. This result is reflected in Fig. 17.
- Figs. 3 and 4 correspond to particular cases in Fig. 17.
- Figs. 5 and 9 can be explained by combining the results in Fig. 17.
- Figs. 8, 12 and 13 were discussed in details above.
- Finally, no phase transition develops in the system when $k_B T/w_{AA} > 0.567$. This is clearly seen in Figs. 6, 7, 10 and 11, where a smooth behavior in the adsorption properties is obtained.

4 Conclusions

Using Monte Carlo simulations, we have studied the adsorption of a gas mixture of interacting particles A and B on homogeneous square surfaces. A variety of behaviors arise due to the formation of different ordered structures in the adlayer for different values of the lateral interactions among adsorbed particles. The analysis of partial and total adsorption isotherms and differential heats of adsorption provides a detailed understanding of the adsorption process. This study yields to the construction of a phase-diagram which allows to understand the critical behavior of the system.

An interesting feature of this work is the occurrence of a minimum in the global adsorption isotherm. This singularity appears as the initial fraction of B particles on the surface is high ($0.4 \leq \theta_B^i \leq 0.5$) and $w_{AB}/k_B T > 0$. This effect might be interesting due to the fact that seems counterintuitive to see a negative slope (therefore a minimum) in the total coverage. Nevertheless, the phenomenon is because the A particles adsorbing in the lattice expel the B particles at a higher ratio; then the partial A [B] coverage increases [decreases] (partial isotherms must cross). In the above regime, the desorbed B particles are more than the adsorbed A particles, therefore we see a total coverage (θ) with a negative slope followed by a minimum.

The computational technique used here has proven to be very powerful tool for these kind of lattice-gas models and many other systems in a much wider scope of sciences, allowing the interpretation of many experimental results without heavy or time-consuming calculations.

5 ACKNOWLEDGMENTS

This work was supported in part by CONICET (Argentina) under project number PIP 112-200801-01332; Universidad Nacional de San Luis (Argentina) under project 322000; Universidad Tecnológica Nacional, Facultad Regional San Rafael (Argentina) under projects PQPRSR 858 and PQCOSR 526 and

the National Agency of Scientific and Technological Promotion (Argentina)
under project 33328 PICT 2005.

Figure Captions

Fig. 1: Adsorption isotherms for the single-gas adsorption of A particles onto the surface showing the effect of lateral AA interactions.

Fig. 2: Mixed-gas adsorption on a square lattice: (a) adsorption isotherms for A and B particles; (b) total adsorption isotherms; (c) differential heat of adsorption for A particles and (d) differential heat of adsorption for B particles. Effect of AA interactions: $w_{AA}/k_B T \geq 0$, $w_{BB}/k_B T = 0$ and $w_{AB}/k_B T = 0$.

Fig. 3: As Fig. 2 for $w_{AA}/k_B T \geq 0$, $w_{BB}/k_B T = 2$ and $w_{AB}/k_B T = 0$.

Fig. 4: As Fig. 2 for $w_{AA}/k_B T \geq 0$, $w_{BB}/k_B T = 0$ and $w_{AB}/k_B T = 2$.

Fig. 5: As Fig. 2 for $w_{AA}/k_B T \geq 0$, $w_{BB}/k_B T = 2$ and $w_{AB}/k_B T = 2$.

Fig. 6: Mixed-gas adsorption on a square lattice: (a) partial adsorption isotherms for A and B particles; (b) total adsorption isotherms; (c) differential heat of adsorption for A particles and (d) differential heat of adsorption for B particles. Effect of AB interactions: $w_{AA}/k_B T = 0$, $w_{BB}/k_B T = 0$ and $w_{AB}/k_B T \geq 0$.

Fig. 7: As Fig. 6 for $w_{AA}/k_B T = 0$, $w_{BB}/k_B T = 2$ and $w_{AB}/k_B T \geq 0$.

Fig. 8: As Fig. 6 for $w_{AA}/k_B T = 5$, $w_{BB}/k_B T = 0$ and $w_{AB}/k_B T \geq 0$.

Fig. 9: As Fig. 6 for $w_{AA}/k_B T = 5$, $w_{BB}/k_B T = 2$ and $w_{AB}/k_B T \geq 0$.

Fig. 10: Mixed-gas adsorption on a square lattice: (a) partial adsorption isotherms for A and B particles; (b) total adsorption isotherms; (c) differential heat of adsorption for A particles and (d) differential heat of adsorption for B particles. Effect of BB interactions: $w_{AA}/k_B T = 0$, $w_{BB}/k_B T \geq 0$ and $w_{AB}/k_B T = 0$.

Fig. 11: As Fig. 10 for $w_{AA}/k_B T = 0$, $w_{BB}/k_B T \geq 0$ and $w_{AB}/k_B T = 2$.

Fig. 12: As Fig. 10 for $w_{AA}/k_B T = 5$, $w_{BB}/k_B T \geq 0$ and $w_{AB}/k_B T = 0$.

Fig. 13: As Fig. 10 for $w_{AA}/k_B T = 5$, $w_{BB}/k_B T \geq 0$ and $w_{AB}/k_B T = 2$.

Fig. 14: Temperature-coverage phase diagram corresponding to a lattice-gas of repulsive monomers ($w_{AA}/k_B T > 0$) adsorbed on a homogeneous square lattice.

Fig. 15: Comparison between the total isotherms in Fig. 13 b) (symbols) and the one corresponding to a square lattice-gas of one species with $w_{AA}/k_B T = 5$ (solid line). The inset shows a snapshot of the $c(2 \times 2)$ phase.

Fig. 16: Effect of the lateral interactions between A-B particles, $w_{AB}/k_B T$, on the temperature-coverage phase diagram corresponding to a binary mixture with $w_{BB}/k_B T = 0$ and $w_{AA}/k_B T$ in the critical regime.

Fig. 17: Densities corresponding to the maxima of the coexistence curves in zone II as a function of (i) $w_{AB}/k_B T$ (solid circles, bottom axis) and (ii) w_{BB} (open circles, upper axis). In case (i) [(ii)], $w_{BB}/k_B T = 0$ [$w_{AB}/k_B T = 0$] and $w_{AA}/k_B T$ is chosen in the critical regime.

References

- [1] D. M. Ruthven, Principles of Adsorption and Adsorption Processes, Wiley, New York, 1984.
- [2] R. T. Yang, Gas Separation by Adsorption Processes, Butterworth, London, 1987.
- [3] L. K. Doraiswamy, Prog. Surf. Sci. 37 (1990) 1.
- [4] W. Rudzinski, W. A. Steele, G. Zgrablich, Equilibria and Dynamics of Gas Adsorption on Heterogeneous Solid Surfaces, Elsevier, Amsterdam, The Netherlands, 1997.
- [5] S. Sircar, Langmuir 7 (1991) 3065.
- [6] M. Heuchel, R. Q. Snurr, E. Buss, Langmuir 13 (1997) 6795.
- [7] K. Ayache, S. E. Jalili, L.J. Dunne, G. Manos, Z. Du, Chem. Phys. Lett. 362 (2002) 414.
- [8] L. J. Dunne, G. Manos, Z. Du, Chem. Phys. Lett. 377 (2003) 551.
- [9] M. Dávila, J. L. Riccardo, A. J. Ramirez-Pastor, J. Chem. Phys. 130 (2009) 174715.
- [10] M. Dávila, J. L. Riccardo, A. J. Ramirez-Pastor, Chem. Phys. Lett. 477 (2009) 402.
- [11] A.L. Myers, Molecular thermodynamics of adsorption of gas and liquid mixtures, in : A. I. Liapis (Ed.), Fundamental of Adsorption, Engineering Foundation, 1987.
- [12] B. Smit, T. L. M. Maesen, Chem. Rev. 108 (2008) 4125.
- [13] F. Gonzalez-Cavallero, M.L. Kerkeb, Langmuir 10 (1994) 1268.
- [14] J. A. Dunne, R. Mariwala, M. Rao, S. Sircar, R. J. Gorte, A. L. Myers, Langmuir 12 (1996) 5888.
- [15] J. A. Dunne, M. Rao, S. Sircar, R. J. Gorte, A. L. Myers, Langmuir 12 (1996) 5896.
- [16] W. A. Steele, The Interaction of Gases with Solid Surfaces, Pergamon Press, New York, 1974.
- [17] E. Alison Flood, The Solid-Gas Interface, M. Dekker Inc., New York, 1967.
- [18] V. P. Zhdanov, Elementary Physicochemical Processes on Solid Surfaces, Plenum Press, New York/London, 1991.
- [19] K. Binder (Ed.), Monte Carlo Methods in Statistical Physics. Topics in Current Physics, vol. 7, Springer, Berlin, 1978.

- [20] K. Binder, Rep. Prog. Phys. 60 (1997) 448.
- [21] K. Binder and D. W. Heermann, Monte Carlo Simulation in Statistical Physics. An Introduction, Springer, Berlin, 1988.
- [22] P. Ungerer, B. Tavitian and A. Boutin, Applications of Molecular Simulation in the Oil and Gas Industry: Monte Carlo Methods, Editions Technip, Paris, 2005.
- [23] F. Bulnes, A.J. Ramirez-Pastor, V.D. Pereyra, J. Mol. Catal. A: Chem 167 (2001) 129.
- [24] D. Nicholson, N. G. Parsonage, Computer Simulation and the Statistical Mechanics of Adsorption, Academic Press, London, 1982.
- [25] F. Bulnes, V. Pereyra, J. L. Riccardo, Phys. Rev. E 58 (1999) 86.
- [26] A. Patrykiewicz, S. Sokolowski, K. Binder, Surf. Sci. Rep. 37 (2000) 207.
- [27] P. Rinaldi, F. Bulnes, A. J. Ramirez-Pastor, G. Zgrablich, Surf. Sci. 602 (2008) 1783.
- [28] Y. K. Tovbin, Application of Lattice-Gas Models to Describe Mixed-Gas Adsorption Equilibria on Heterogeneous Solid Surfaces, in: W. Rudzinski, W. A. Steele, G. Zgrablich (Eds.), Equilibria and Dynamics of Gas Adsorption on Heterogeneous Solid Surfaces, Elsevier, Amsterdam, 1996.
- [29] H. A. Kramers, G. H. Wannier, Phys. Rev. B 60 (1941) 252.
- [30] J.M. Yeomans, Statistical Mechanics of Phase Transitions, Clarendon Press, Oxford, 1992.
- [31] A.J. Ramirez-Pastor, F. Bulnes, Physica. A 283 (2000) 198.
- [32] F. Bulnes, A. J. Ramirez-Pastor, G. Zgrablich, Adsorp. Sci. Technol. 23 (2005) 81.
- [33] J. Jiang, S. I. Sandler, M. Schenk, B. Smit, Phys. Rev. B 72 (2005) 045447.
- [34] J. Jiang, S. I. Sandler, Langmuir 22 (2006) 5702.
- [35] L. Onsager, Phys. Rev. 65 (1944) 117.

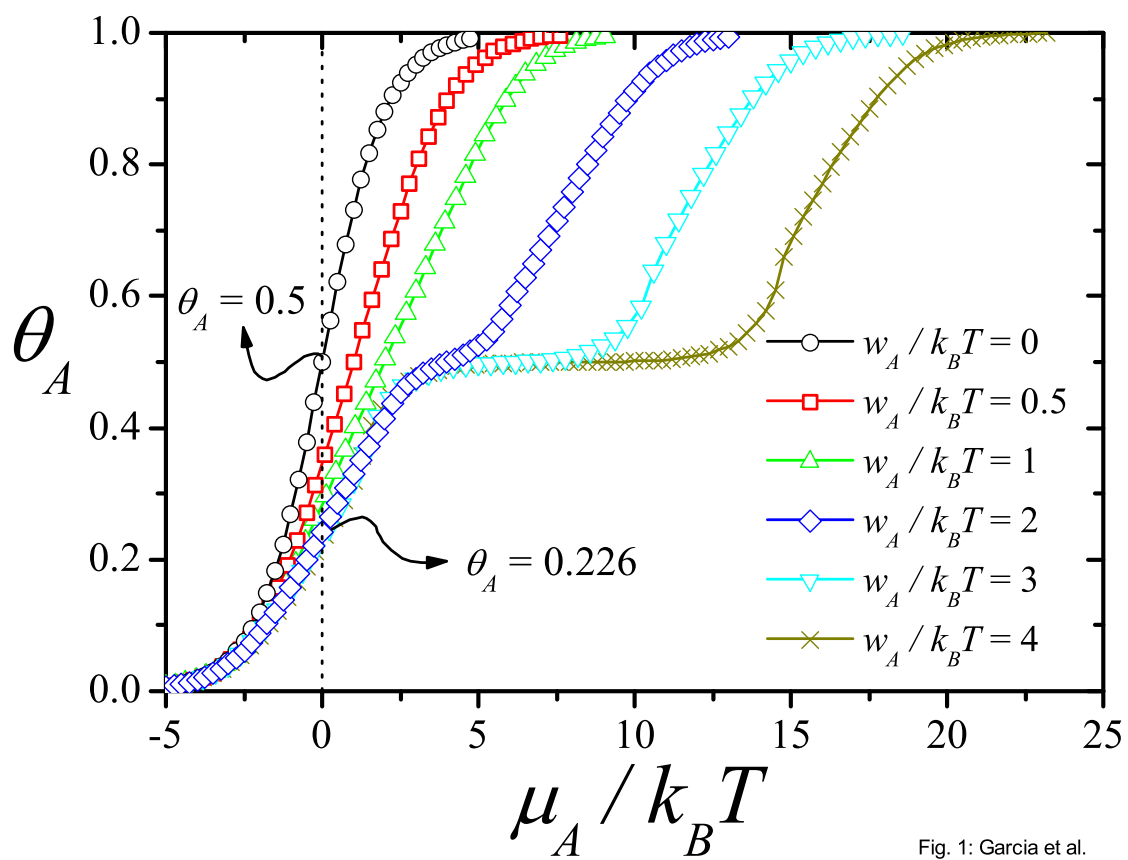


Fig. 1: Garcia et al.

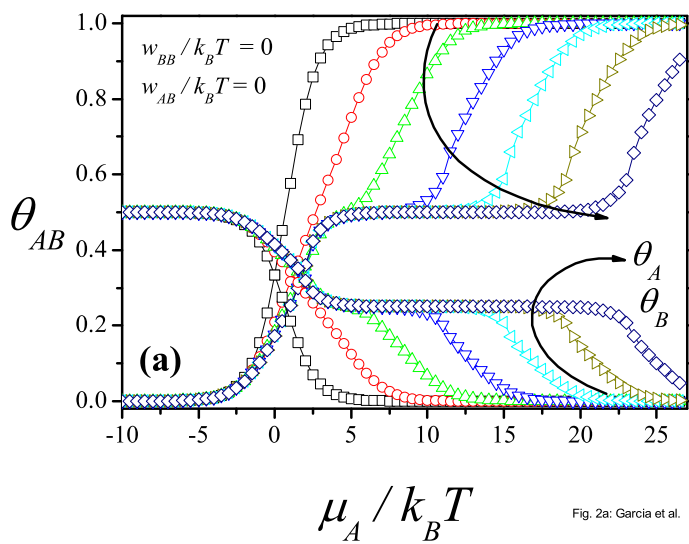


Fig. 2a: Garcia et al.

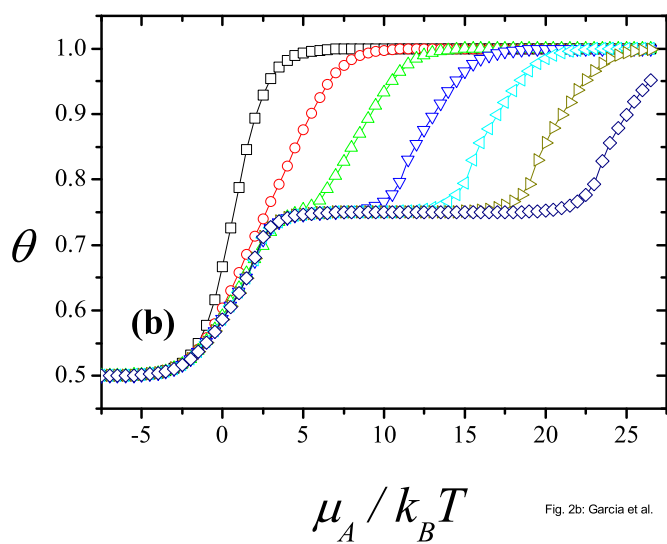


Fig. 2b: Garcia et al.

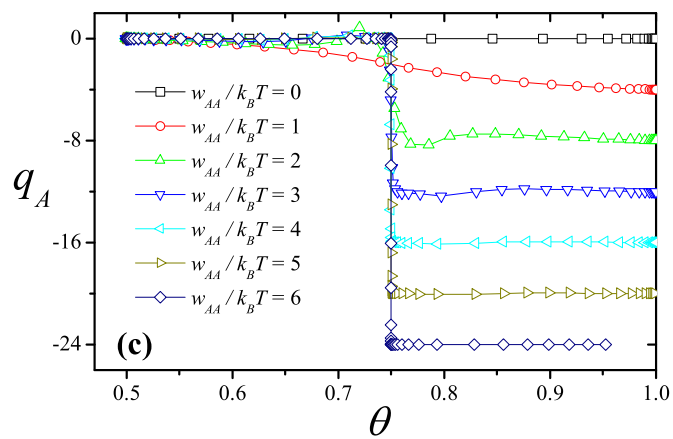


Fig. 2c: Garcia et al.

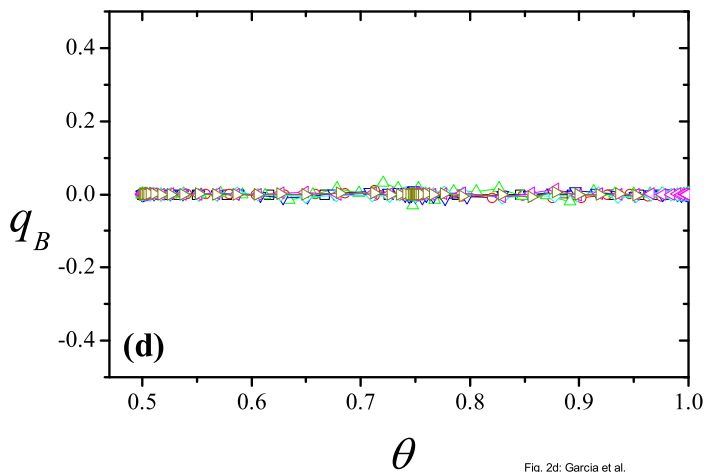


Fig. 2d: Garcia et al.

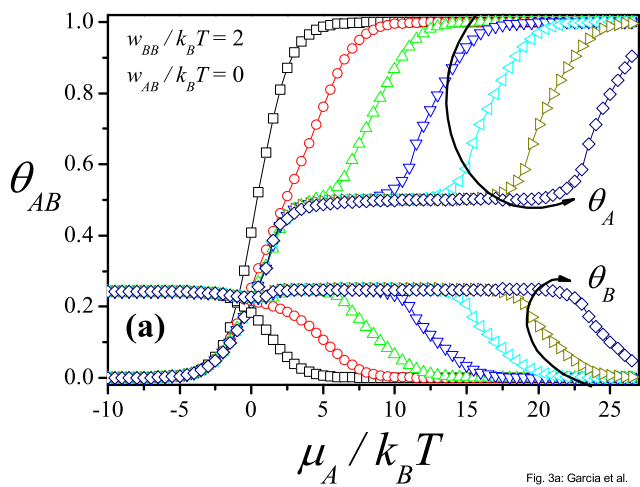


Fig. 3a: Garcia et al.

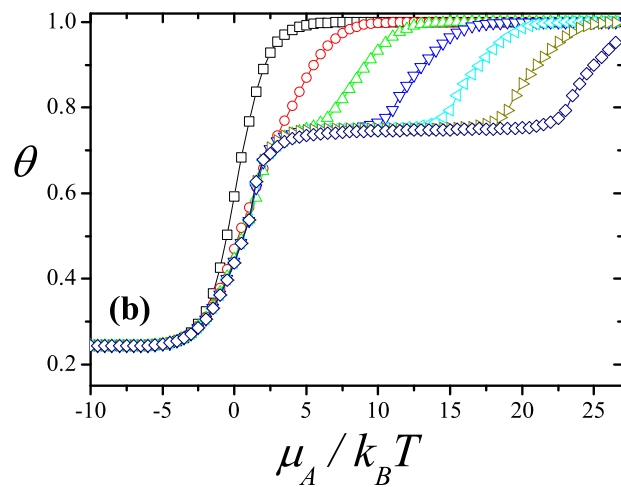


Fig. 3b: Garcia et al.

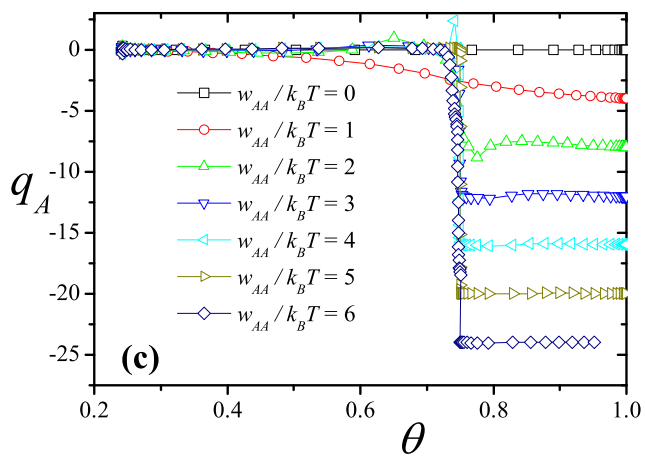


Fig. 3c: Garcia et al.

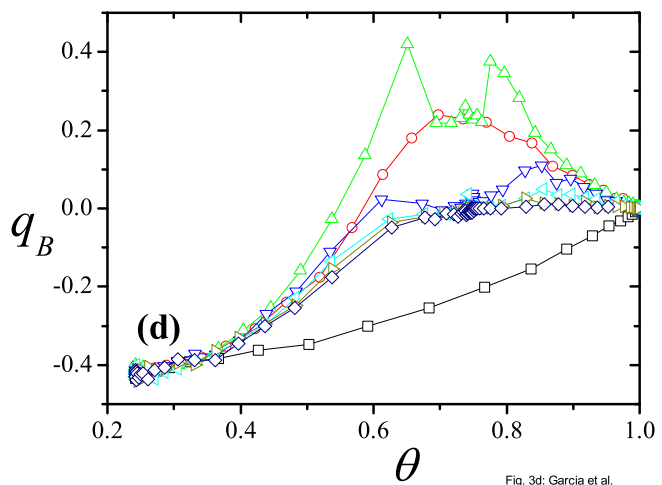


Fig. 3d: Garcia et al.

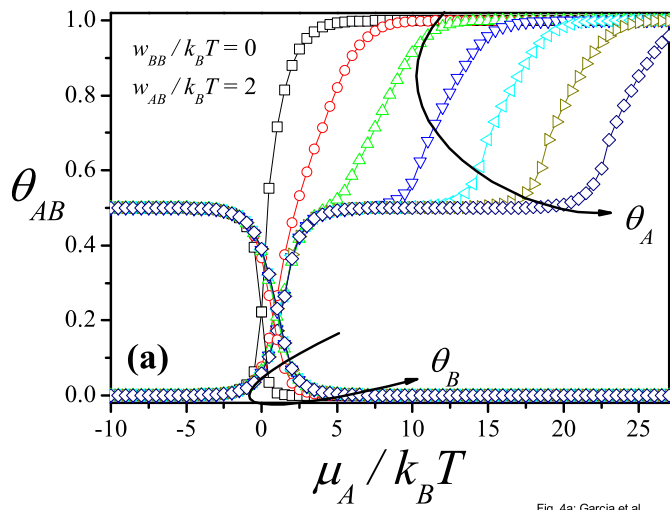


Fig. 4a: Garcia et al.

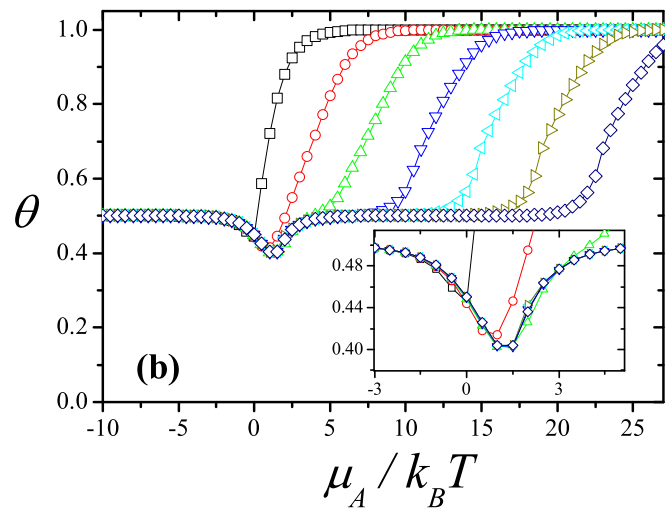


Fig. 4b: Garcia et al.

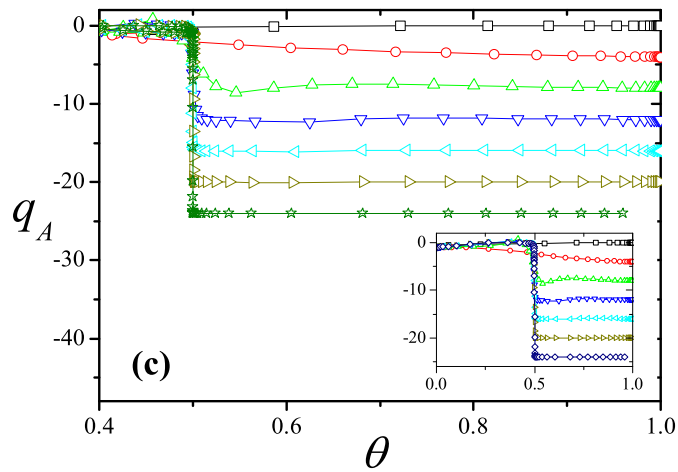


Fig. 4c: Garcia et al.

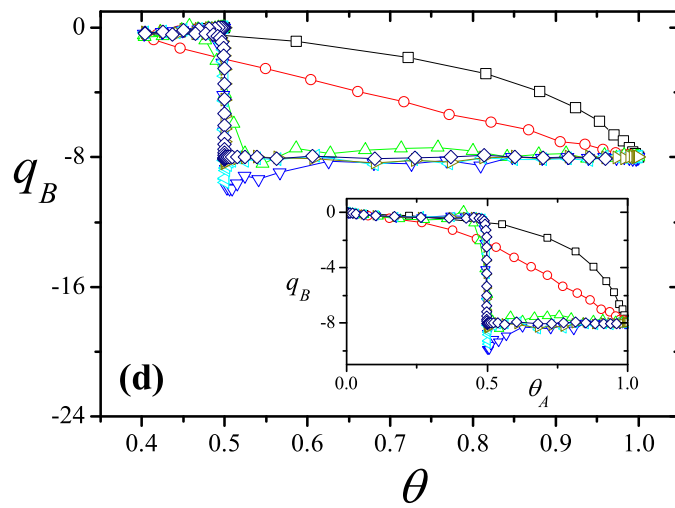


Fig. 4d: Garcia et al.

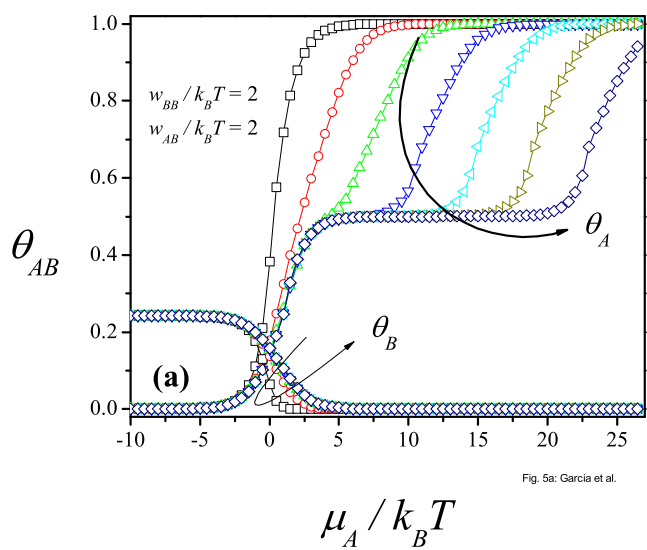


Fig. 5a: García et al.

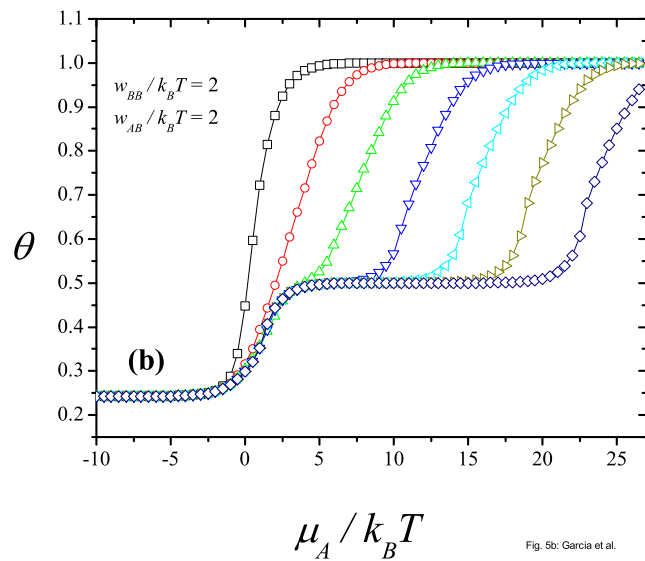


Fig. 5b: García et al.

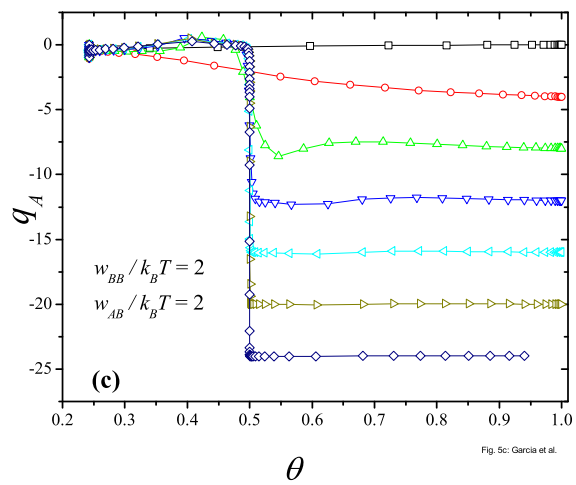


Fig. 5c: García et al.

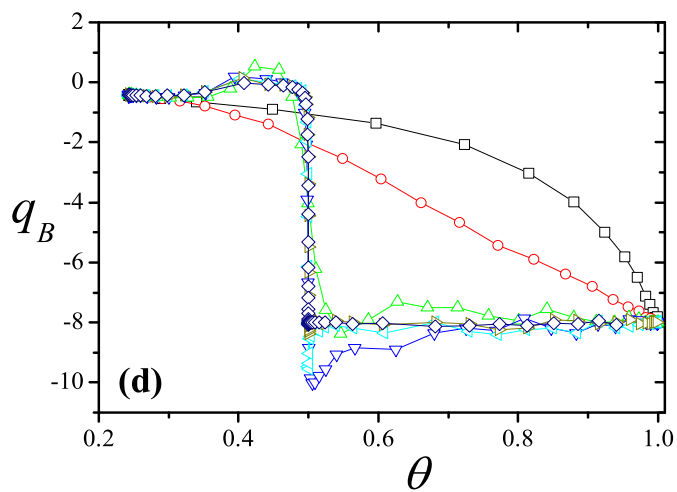


Fig. 5d: García et al.

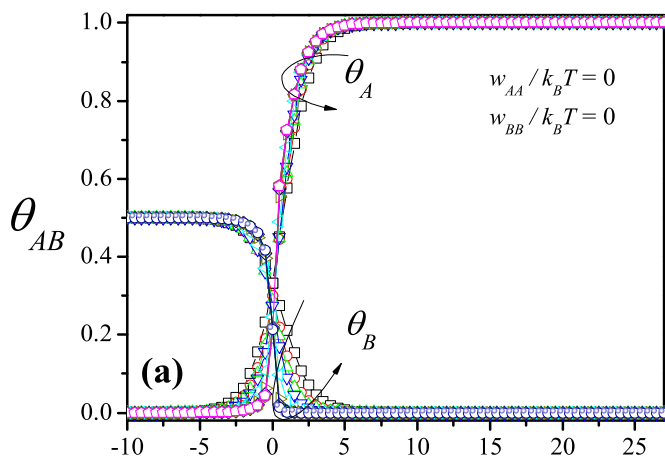


Fig. 6a: Garcia et al.

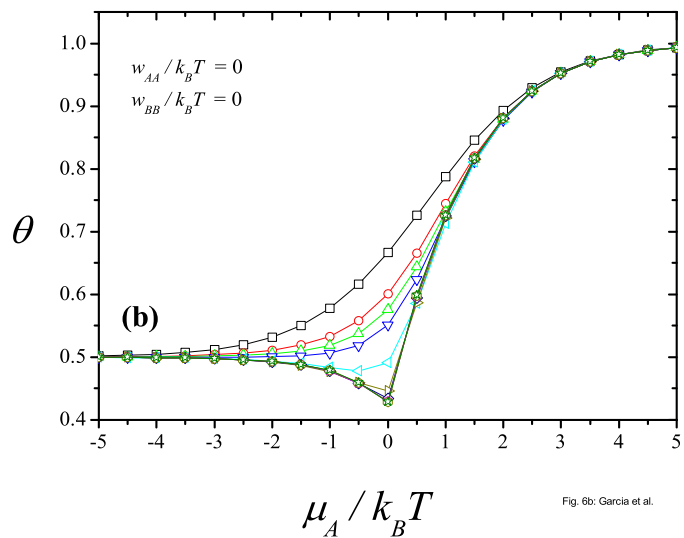


Fig. 6b: Garcia et al.

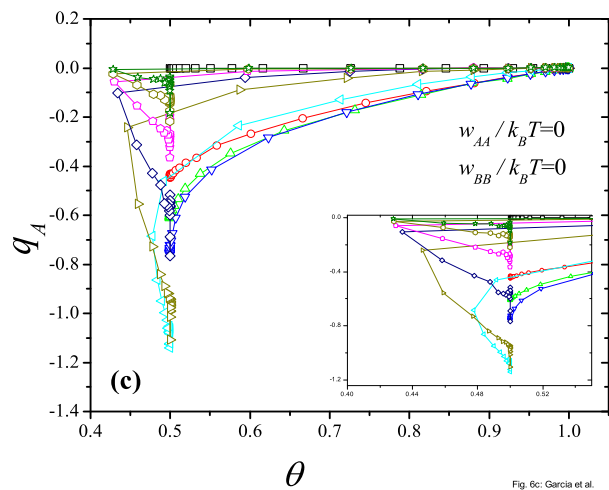


Fig. 6c: Garcia et al.

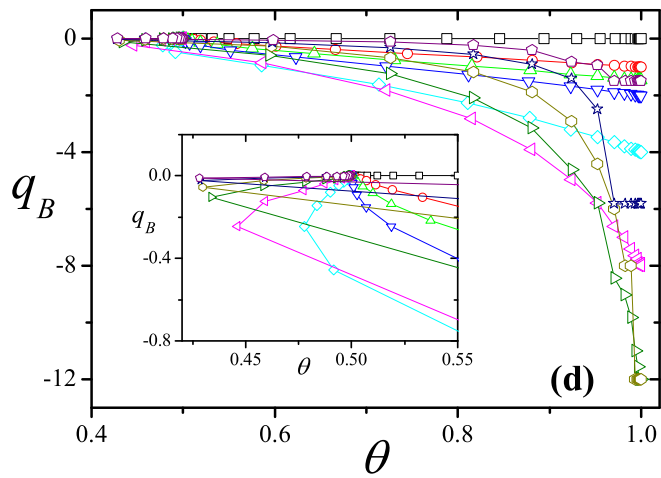


Fig. 6d: Garcia et al.

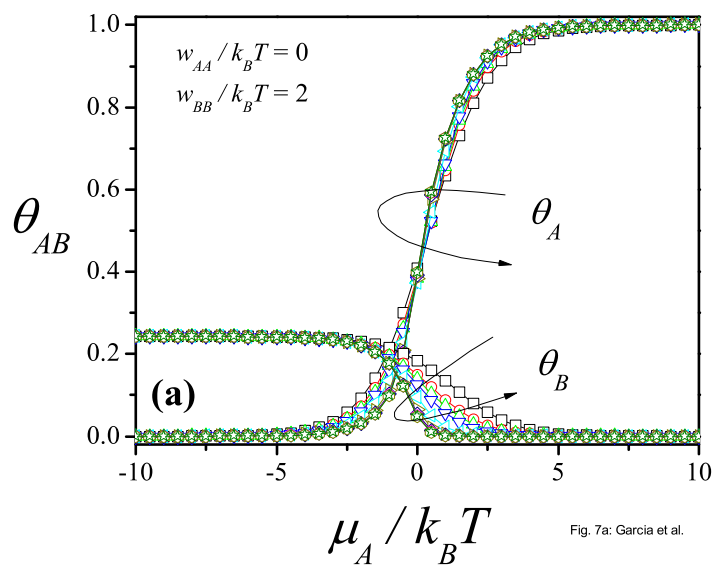


Fig. 7a: García et al.

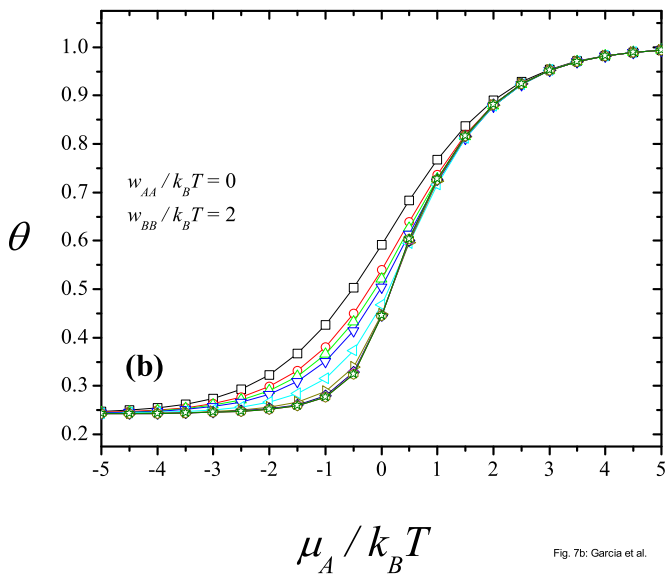


Fig. 7b: García et al.

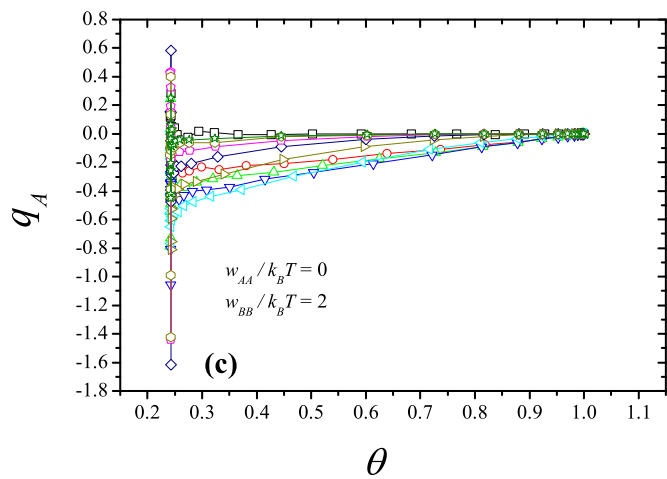


Fig. 7c: García et al.

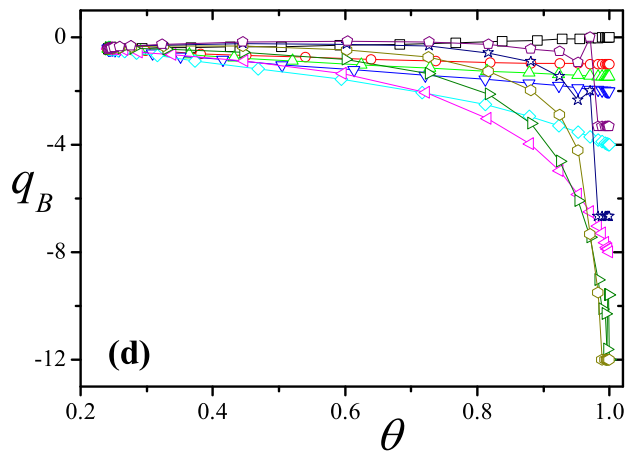


Fig. 7d: García et al.

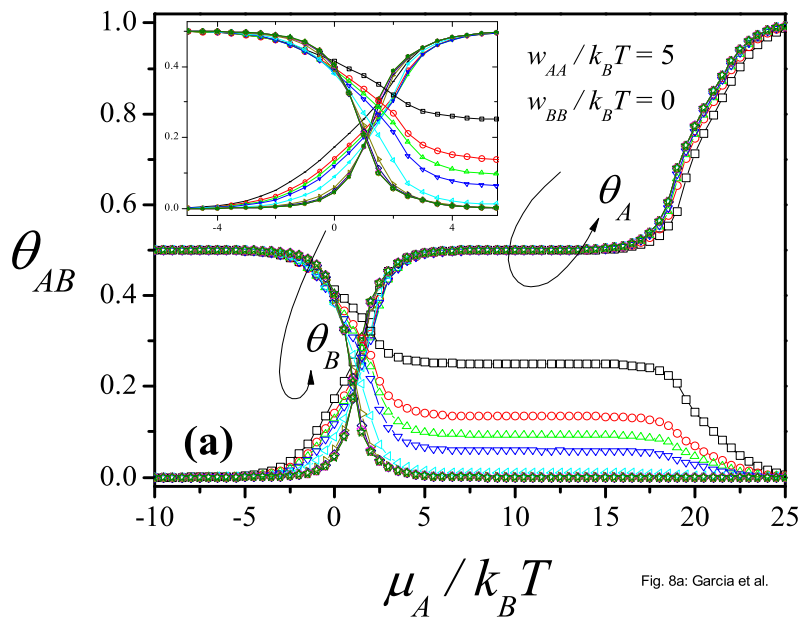


Fig. 8a: Garcia et al.

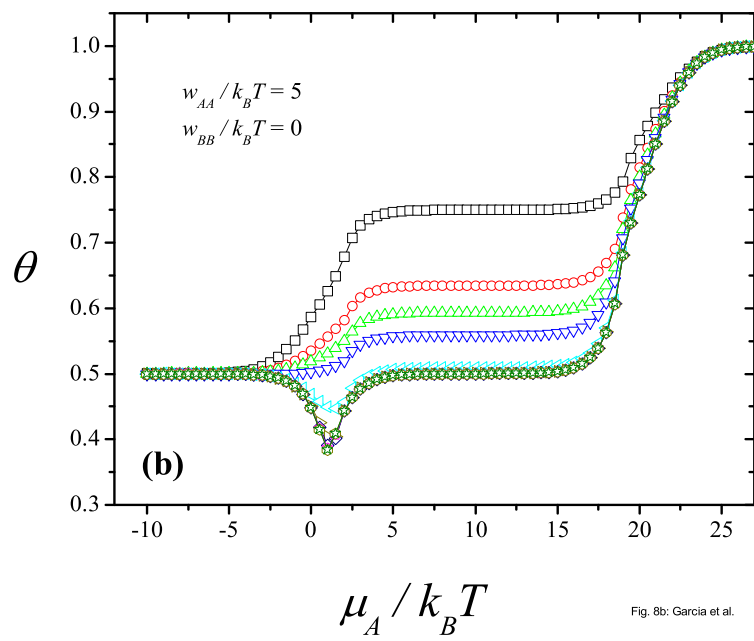


Fig. 8b: Garcia et al.

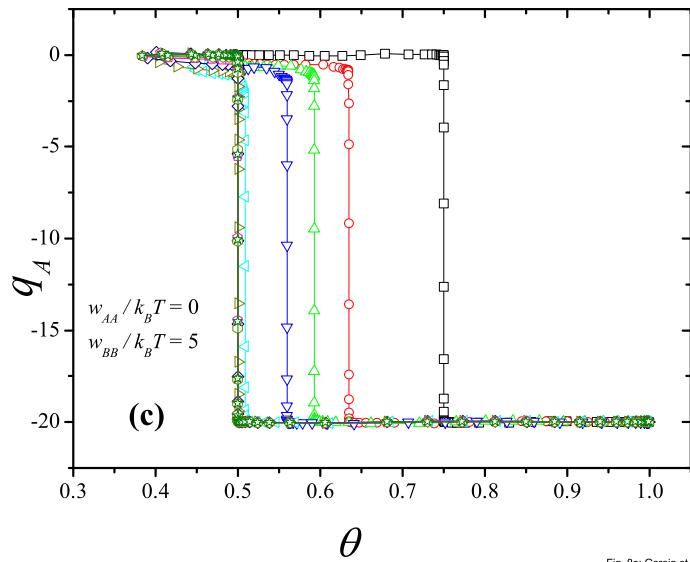


Fig. 8c: Garcia et al.

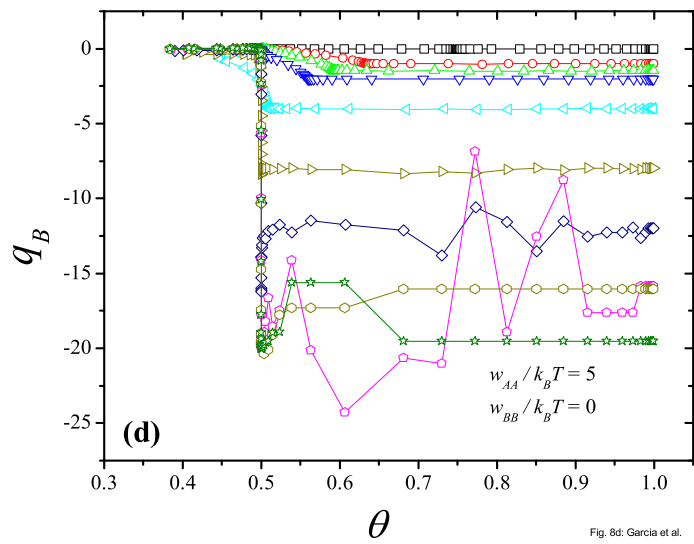


Fig. 8d: Garcia et al.

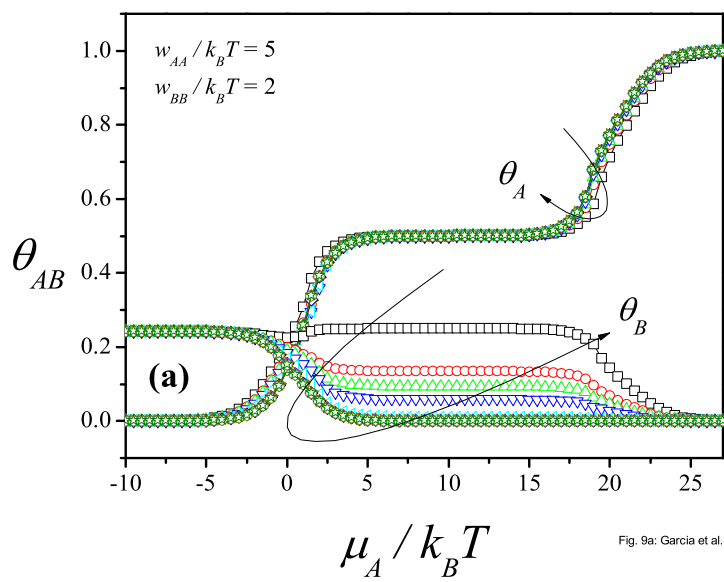


Fig. 9a: Garcia et al.

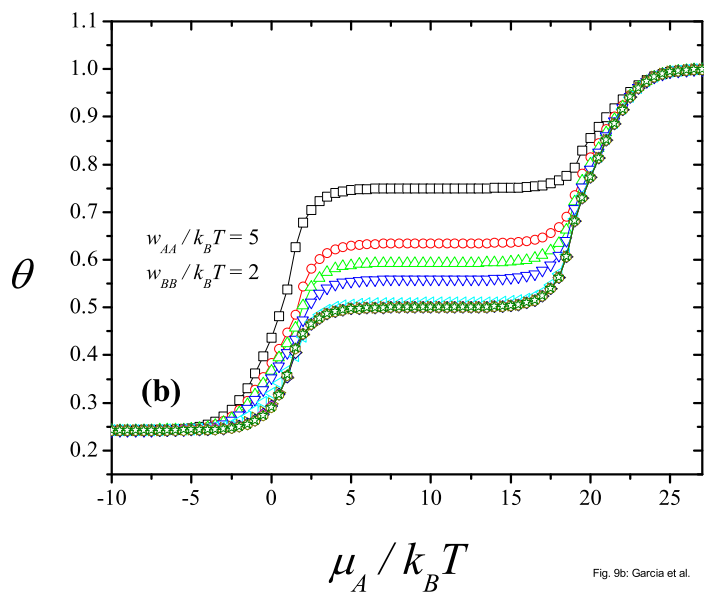


Fig. 9b: Garcia et al.

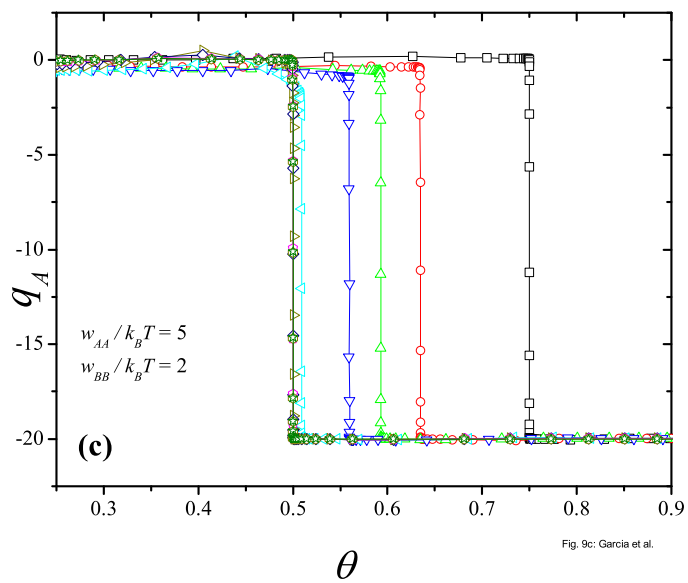


Fig. 9c: Garcia et al.

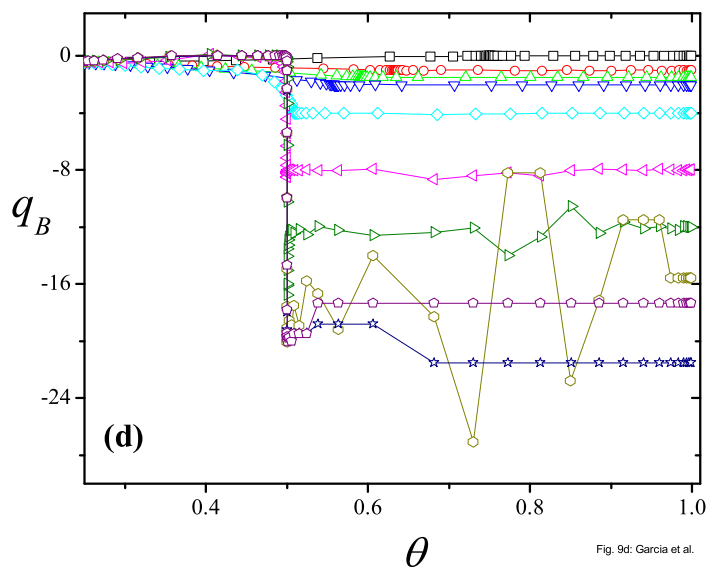


Fig. 9d: Garcia et al.

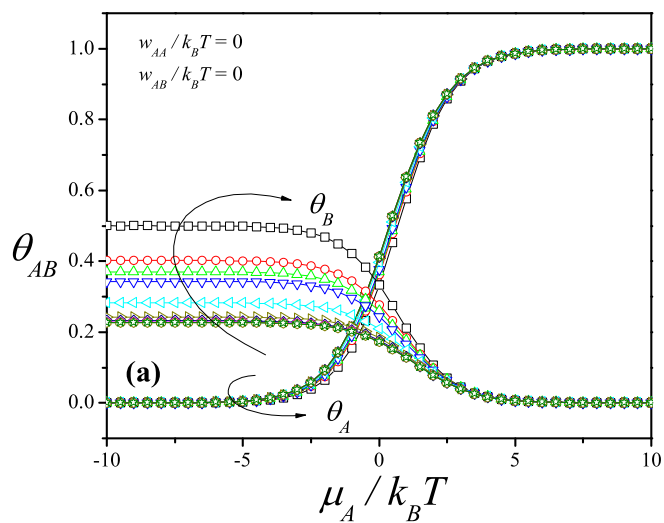


Fig. 10a: Garcia et al.

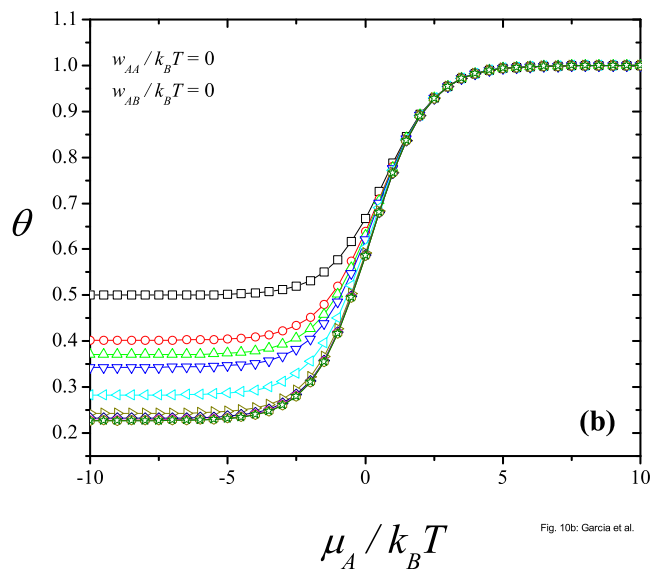


Fig. 10b: Garcia et al.

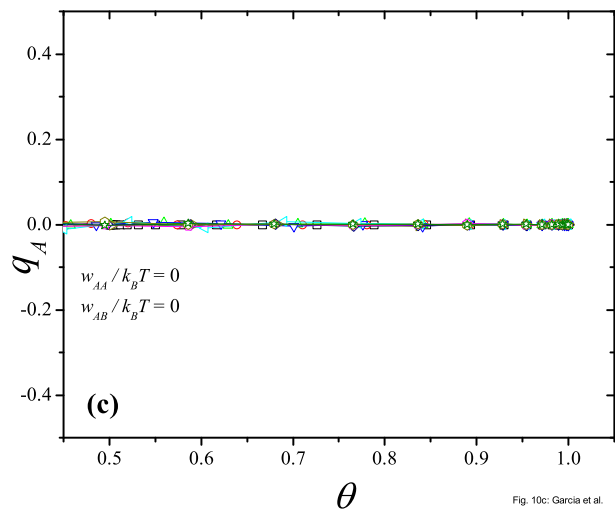


Fig. 10c: Garcia et al.

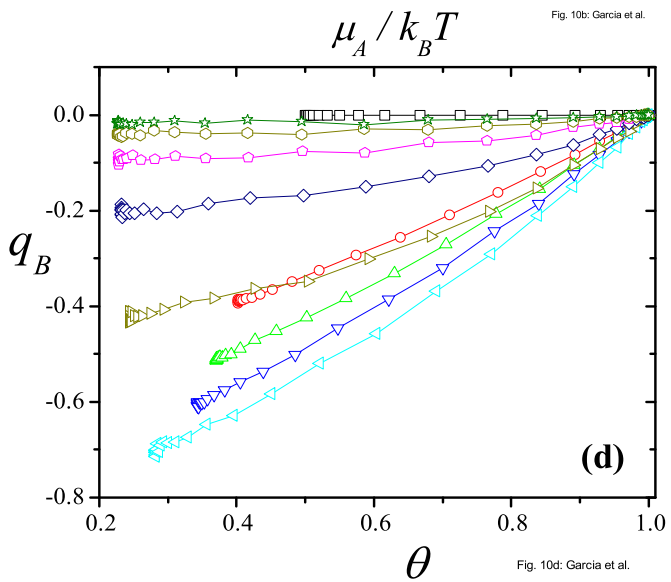


Fig. 10d: Garcia et al.

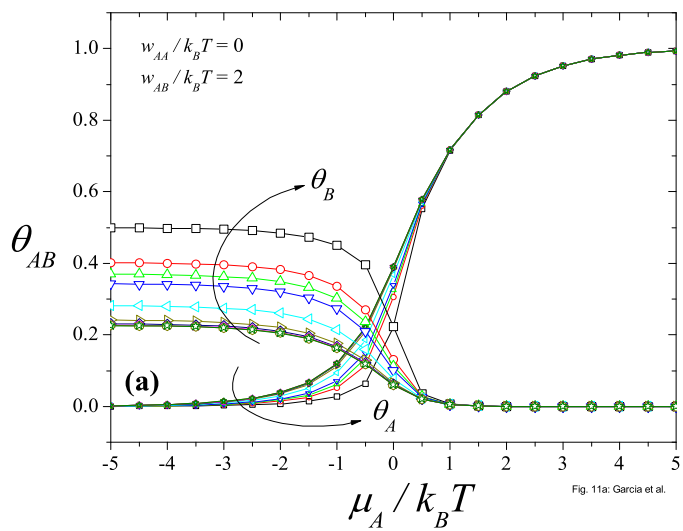


Fig. 11a: Garcia et al.

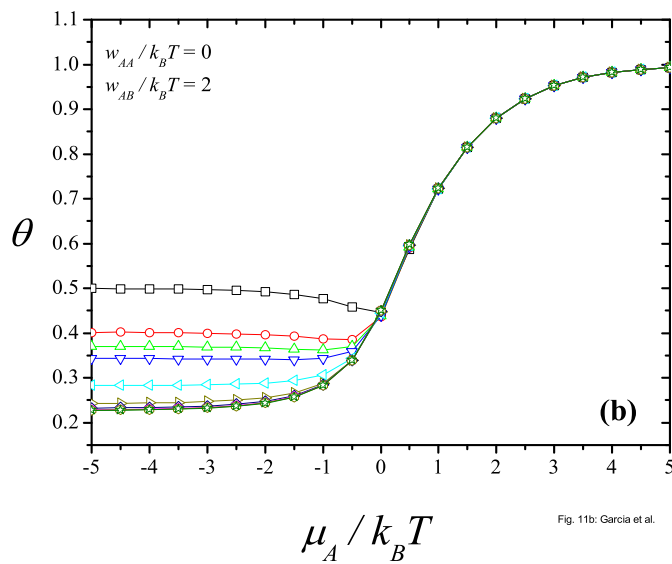


Fig. 11b: Garcia et al.

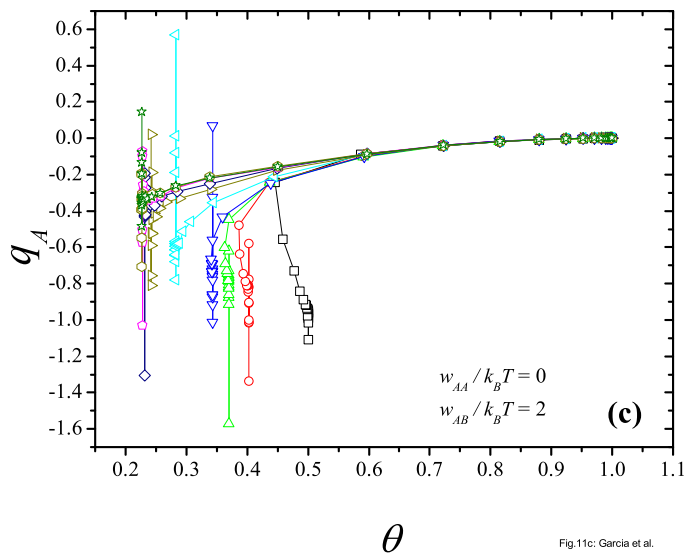


Fig. 11c: Garcia et al.

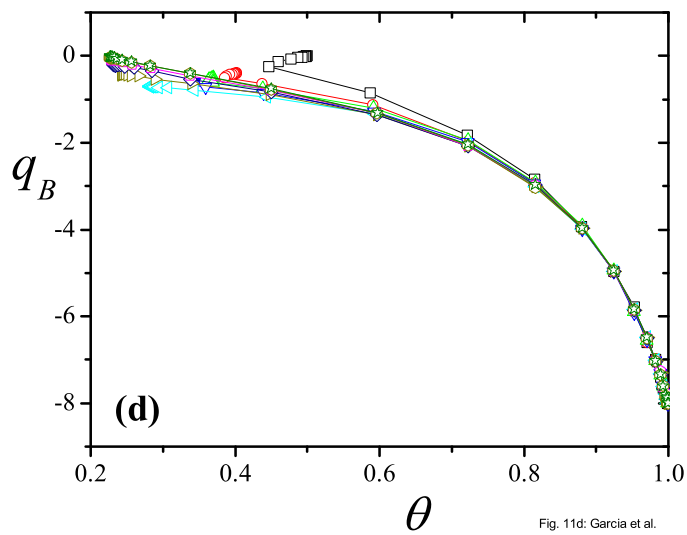


Fig. 11d: Garcia et al.

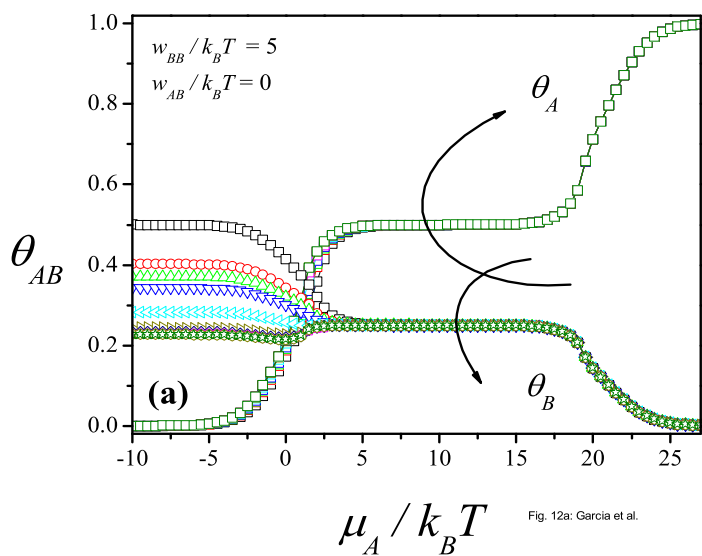


Fig. 12a: Garcia et al.

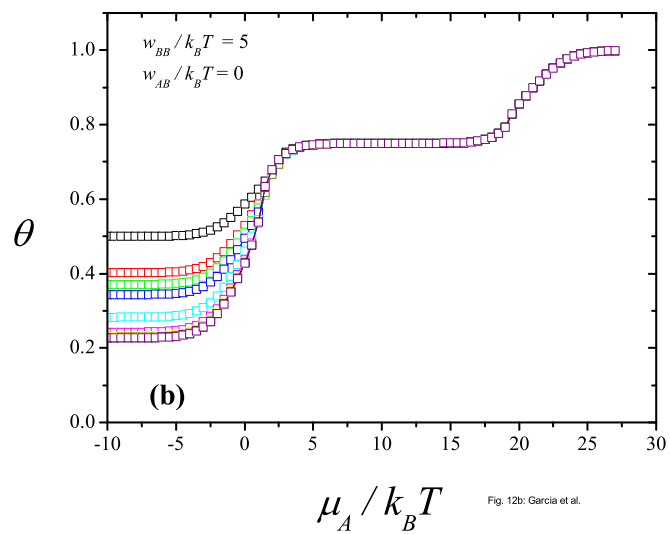


Fig. 12b: Garcia et al.

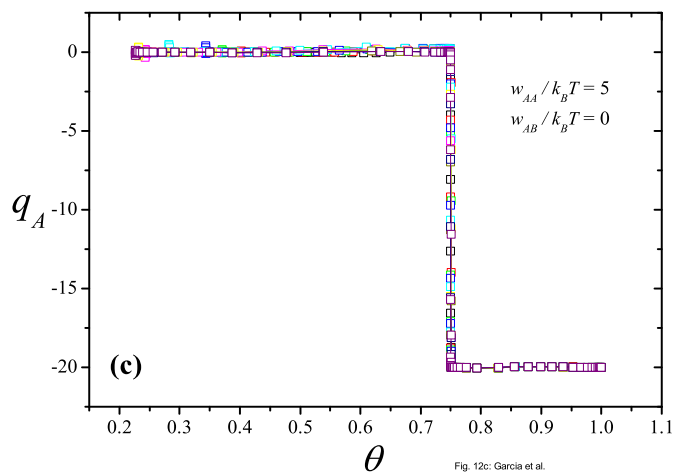


Fig. 12c: Garcia et al.

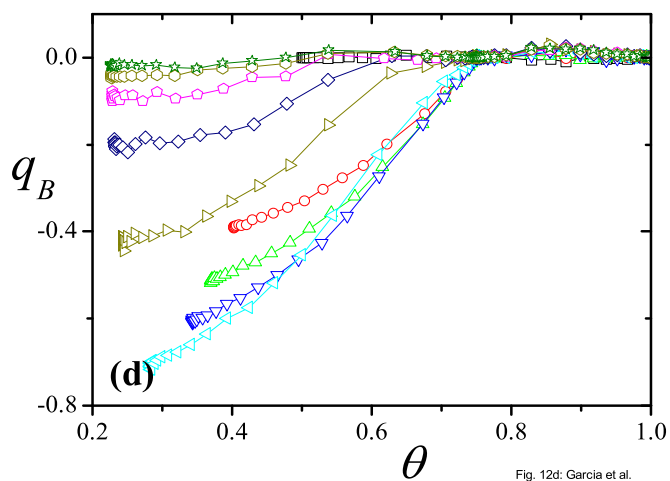


Fig. 12d: Garcia et al.

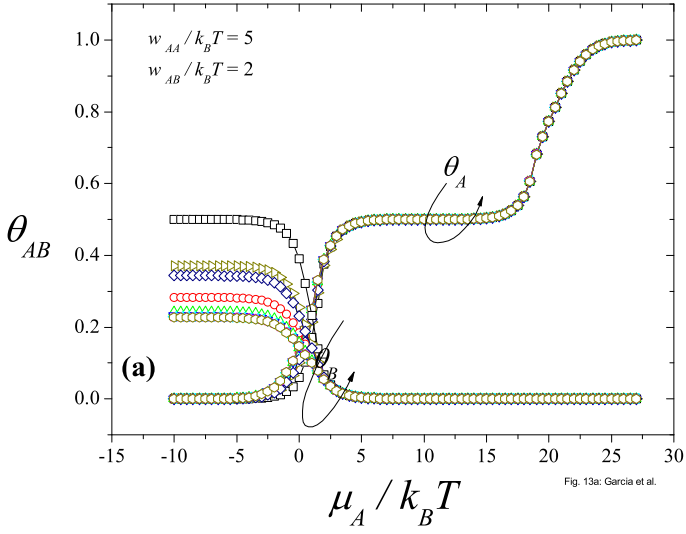


Fig. 13a: Garcia et al.

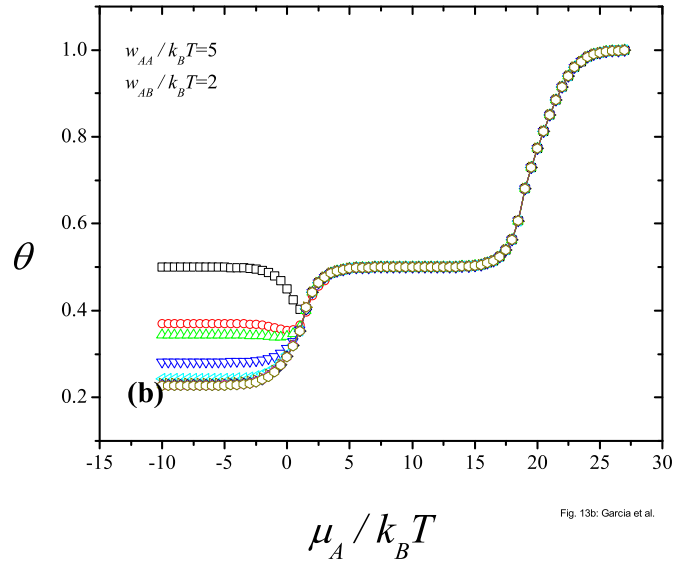


Fig. 13b: Garcia et al.

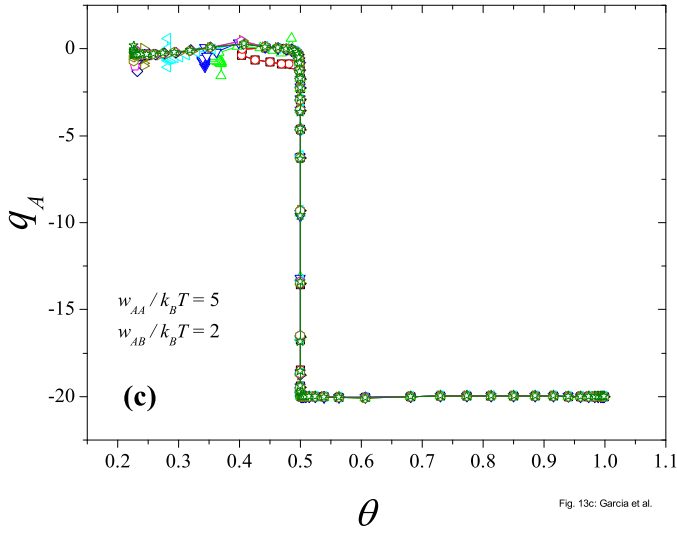


Fig. 13c: Garcia et al.

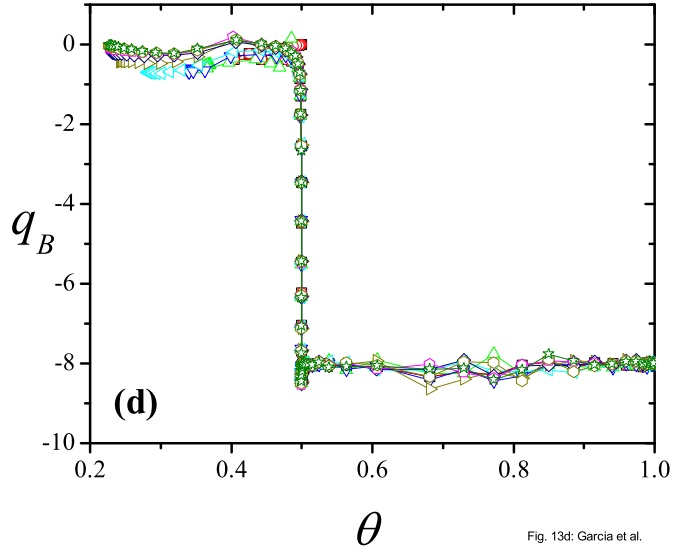


Fig. 13d: Garcia et al.

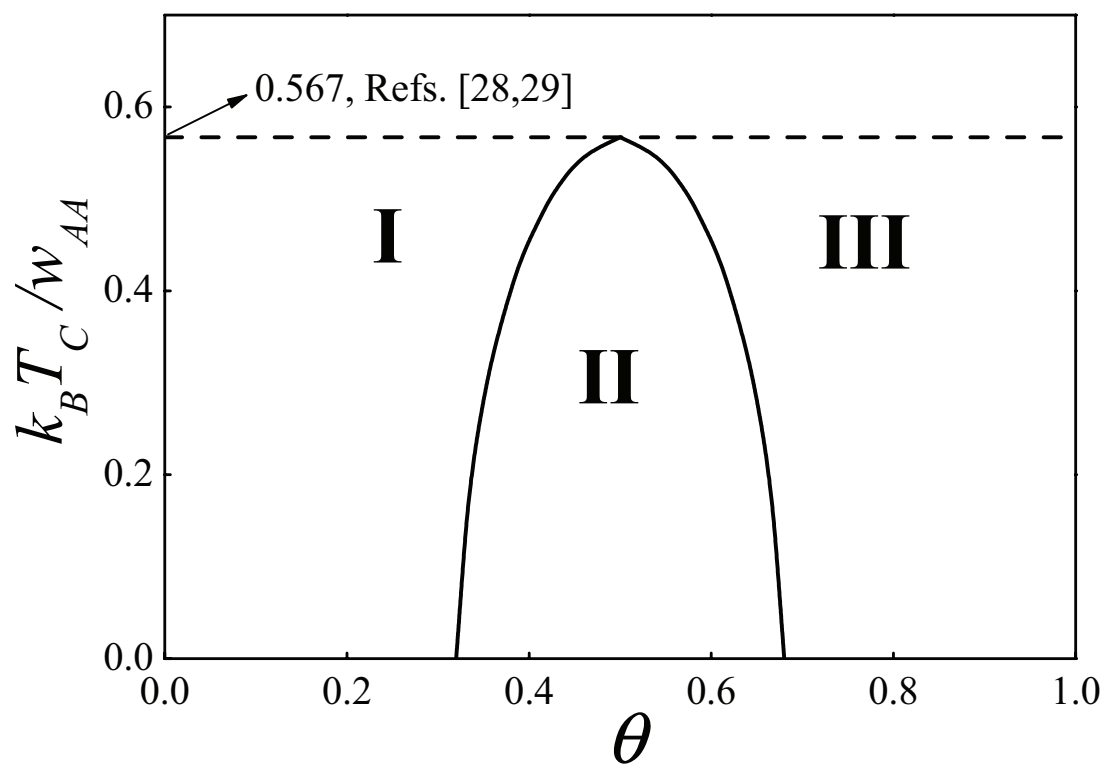


Fig. 14: Garcia et al.

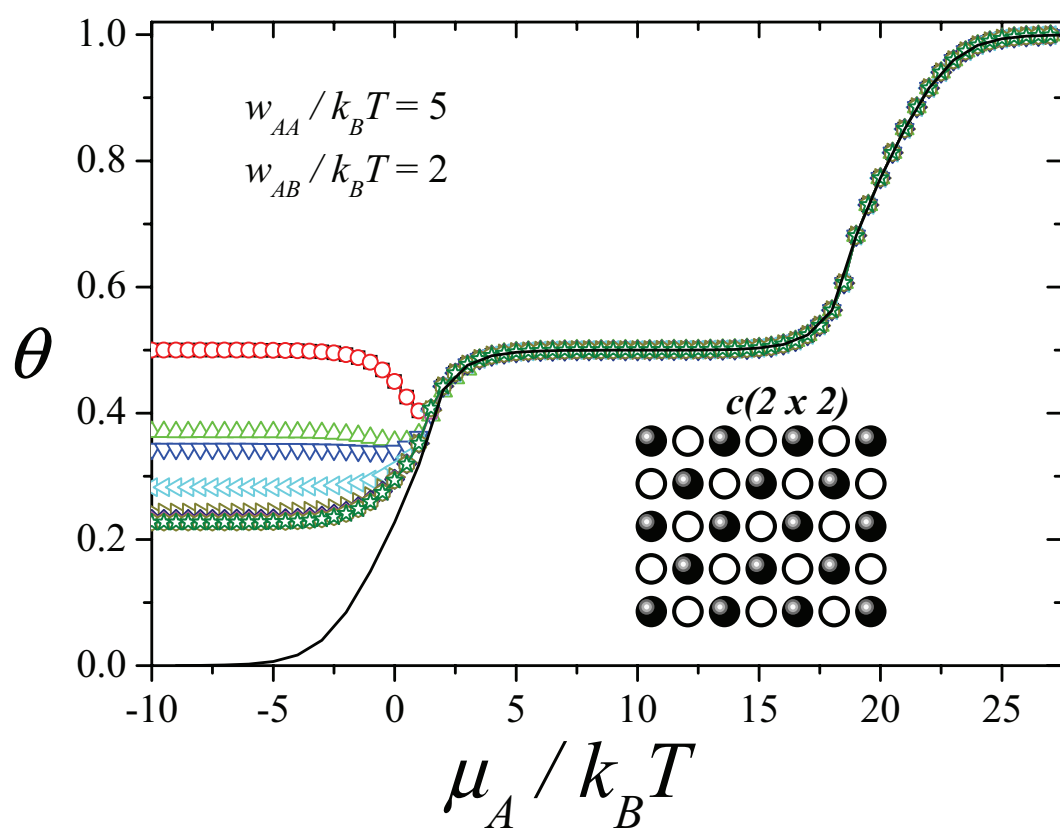


Fig. 15: Garcia et al.

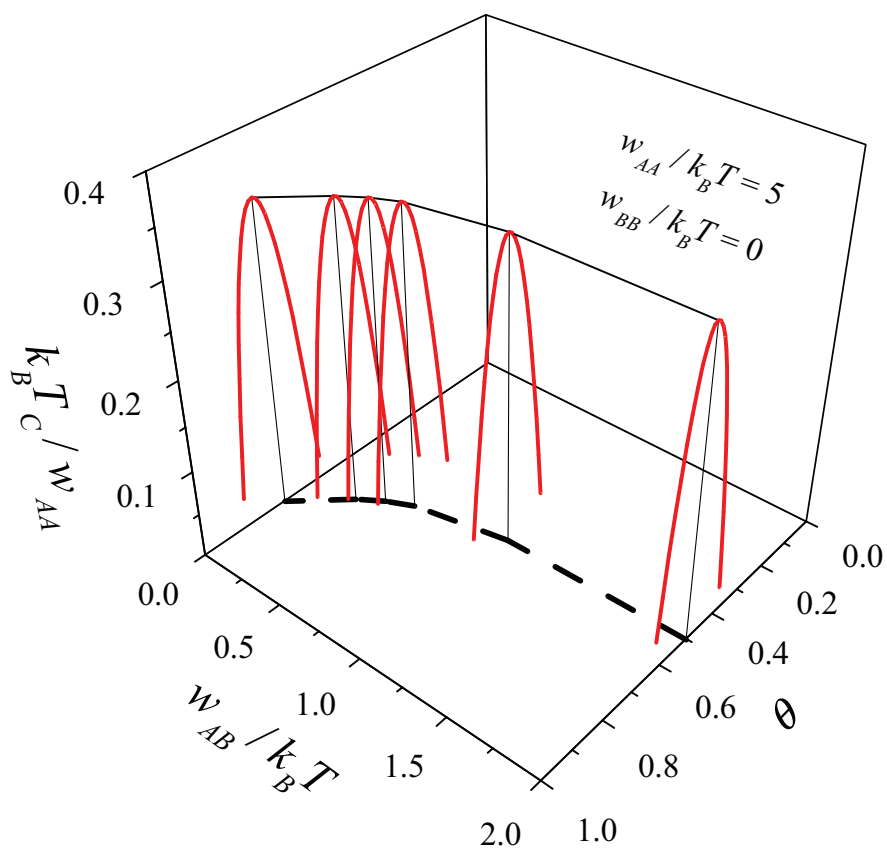


Fig. 16: Garcia et al.

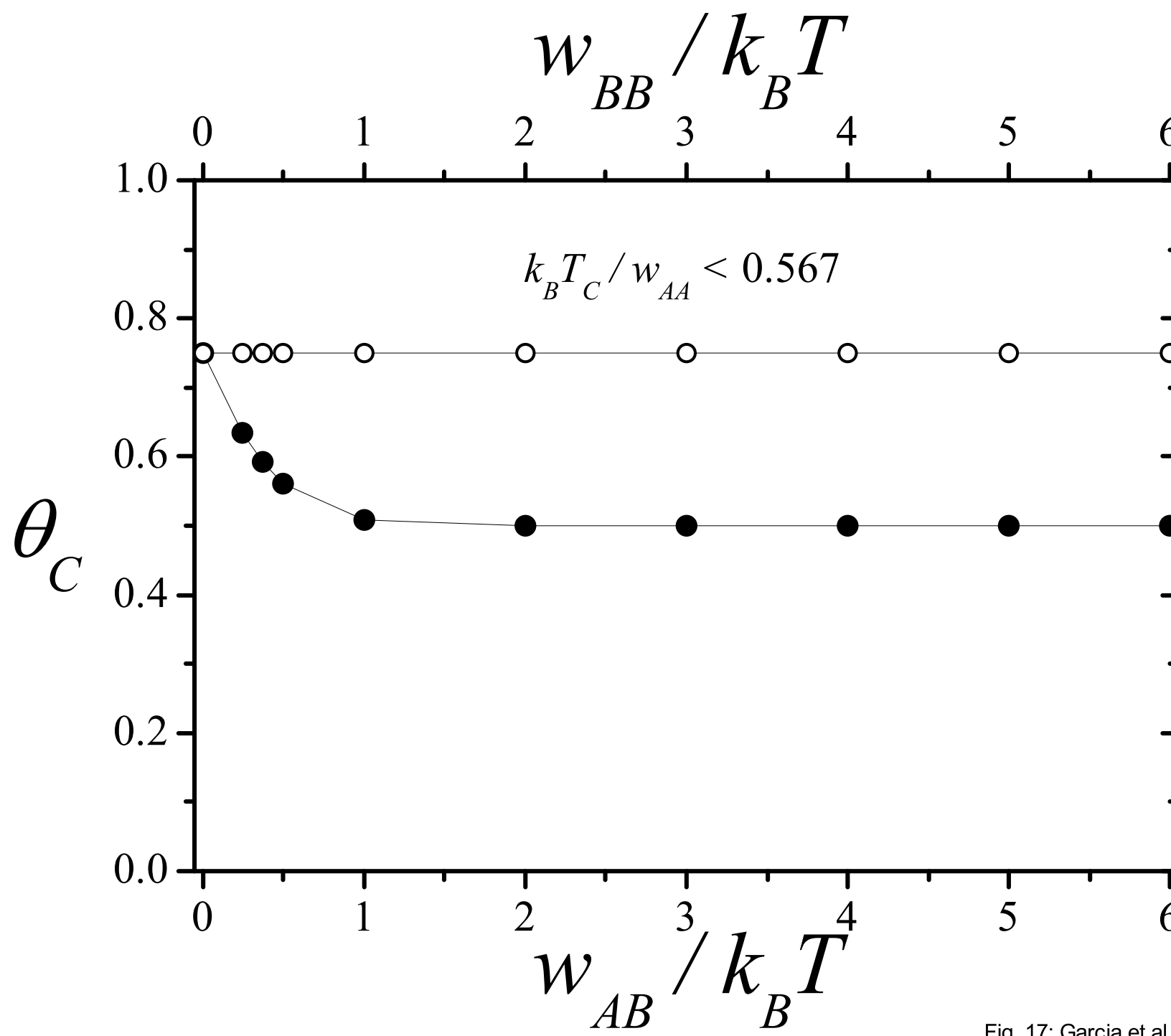


Fig. 17: Garcia et al.